analytical chemistry

Article

pubs.acs.org/ac

Plasmonic Hepatitis B Biosensor for the Analysis of Clinical Saliva

Tomáš Riedel,*[,†] Simone Hageneder,[‡] František Surman,[†] Ognen Pop-Georgievski,[†] Christa Noehammer,[§] Manuela Hofner,[§] Eduard Brynda,[†] Cesar Rodriguez-Emmenegger,*[,†,∥] and Jakub Dostálek*[,‡]

[†]Institute of Macromolecular Chemistry AS CR v.v.i., Heyrovsky Sq. 2, 162 06 Prague 6, Czech Republic

[‡]Biosensor Technologies, AIT-Austrian Institute of Technology GmbH, Muthgasse 11, 1190 Vienna, Austria

[§]Molecular Diagnostics, Health and Environment Department, AIT-Austrian Institute of Technology GmbH, Muthgasse 11, 1190 Vienna, Austria

[∥]DWI – Leibniz Institute for Interactive Materials and Institute of Technical and Macromolecular Chemistry, RWTH Aachen University, Forckenbeckstraße 50, 52074 Aachen, Germany

Supporting Information

ABSTRACT: A biosensor for the detection of hepatitis B antibodies in clinical saliva was developed. Compared to conventional analysis of blood serum, it offers the advantage of noninvasive collection of samples. Detection of biomarkers in saliva imposes two major challenges associated with the low analyte concentration and increased surface fouling. The detection of minute amounts of hepatitis B antibodies was performed by plasmonically amplified fluorescence sandwich immunoassay. To have access to specific detection, we prevented the nonspecific adsorption of biomolecules present in saliva by brushes of poly[(*N*-(2-hydroxypropyl) methacrylamide)-*co*-(carboxybetaine methacrylamide)] grafted from the gold sensor surface and post modified with hepatitis B surface antigen. Obtained results were validated against the response measured with ELISA at a certified laboratory using serum from the same patients.

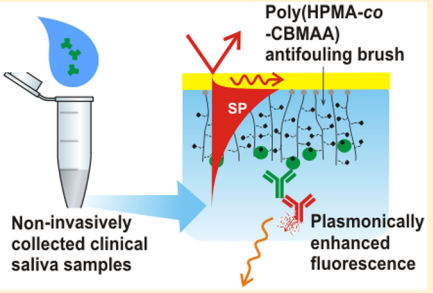

Analytical tests that become available for detection of a broad spectrum of molecular biomarkers in blood plasma or serum provide a powerful tool for diagnosis of diseases. However, the invasive nature of blood collection complicates the analysis for special populations (e.g., elderly people, small children) and in situations when blood sampling is not possible or patients impose high risk of infection. Noninvasive sample collection holds potential to solve this problem, bring the analysis closer to the patient, and set the basis for point-of-care analysis with increased frequency of individual tests, thus enhancing the chances for early diagnosis.

The use of easily accessible bodily fluids, in particular the use of saliva, is an attractive alternative to blood as a large number of disease biomarkers are also present in this fluid and its collection is inexpensive, completely noninvasive, and minimally disturbing for the patient.[1] Saliva is a complex fluid containing a variety of glycoproteins, antibodies, growth factors, carbohydrates, salts, hormones, mucus, and bacteria that leach from blood by passive, as well as active transport.[2] In the past, saliva had already been used to monitor oral health and periodontal diseases.[3] With the advance of modern biochemical techniques more biomarkers for systemic diseases were identified in saliva.[4]

Specific antibodies against epitopes displayed on the capside of the hepatitis B virus (hepatitis B surface antigen-HBsAg) are secreted to blood upon infection or vaccination. The evaluation of the presence of antibodies against HBsAg (anti-HBs) in serum allows confirming the recovery and immunity in patients, as well as checking for the efficiency of vaccination.[5] Hepatitis B virus (HBV) can cause potentially life-threatening diseases, such as chronic hepatitis, cirrhosis, or even liver cancer, and therefore, it represents one of the major global health threats. Especially in African countries, HBV is highly prevalent and causes rising infections[6] that are associated with about 0.8 million deaths every year related to hepatitis B.[7] HBV can be easily transmitted by the contact with infected blood or body fluids.[8]

The use of saliva as a diagnostic tool for the analysis of biomarkers actively or passively transferred from blood (such as anti-HBs) is challenging as they are typically present at concentrations several orders of magnitude lower than in plasma, and thus it requires platforms with substantially enhanced sensitivity.[9−11] Plasmonics has recently emerged as new nanophotonics research field that provides sensitive means for direct label-free detection of biomarkers.[12] In addition, plasmonics increasingly finds its application for the amplification of weak optical signals in optical spectroscopy-based analytical techniques.[13] Among these, plasmonic amplification of fluorescence paved new ways for advancing single molecule studies.[14] In addition, it has been increasingly applied in optical systems that employ fluorescence readout of assays relying on ensembles

Received: November 10, 2016
Accepted: February 7, 2017
Published: February 7, 2017

DOI: 10.1021/acs.analchem.6b04432
Anal. Chem. 2017, 89, 2972−2977

of fluorophores coupled with biomolecules.[15,16] The plasmon-enhanced fluorescence (PEF) that is also referred to as metal-enhanced fluorescence (MEF) exploits the extremely strong electromagnetic field intensity that occurs upon the resonant excitation of surface plasmons (SPs) at metallic nanostructures and on thin metal films. This phenomenon originates from collective oscillations of electron density at these structures and they enable increasing the intensity of emitted fluorescence light from emitters in their close proximity. When fluorophores are used as labels in immunoassays, their coupling with SPs enhances the fluorescence light intensity extracted from the surface where the assay takes place. This type of amplification thus allows resolving lower amount of captured target molecules and concomitantly improving the limit of detection of an assay.

In spite of high sensitivity of plasmonic biosensors that enable reaching limit of detection < fM concentrations,[12] we witnessed limited success in translation of these systems to clinical praxis. For example, several hepatitis plasmonic biosensor system utilizing label-free surface plasmon resonance (SPR) detection of binding induced refractive index changes were developed.[17,18] However, these biosensors were typically applied only for the analysis of model samples such as spiked buffer or pooled diluted serum. Arguably, the key problem in the analysis of clinically relevant samples by plasmonic biosensors is the fouling of their metallic surface with tethered ligands for specific capture of target analyte.[19,20] To solve this problem, research in surface chemistries and architectures was pursued to decrease or completely eliminate the adverse effect of fouling and thereby maximize the efficiency. The most widely used surface modifications are based on poly(ethylene glycol) (PEG), for example, self-assembled monolayers (SAM) terminated with short oligoethylene glycol (OEG). While this approach is able to completely eliminate the nonspecific adsorption of albumin, it fails when complex samples (such as blood plasma/serum and saliva) are analyzed.[21,22]

In this work, a biosensor for the noninvasive analysis of anti-HBs antibodies in clinical saliva samples is presented. It takes advantage of highly sensitive plasmon-enhanced fluorescence readout and novel antifouling poly[(*N*-(2-hydroxypropyl) methacrylamide)-*co*-(carboxybetaine methacrylamide)] (poly-[HPMA-*co*-CBMAA]) polymer brush. This recently developed brush retains its properties even after the immobilization of large surface mass density of ligands.[23] This combination addresses the two key challenges in the biomarker analysis in saliva that are associated with extremely low analyte concentration and severe unspecific interactions with the biosensor surface.

EXPERIMENTAL SECTION

Materials. 1-Ethyl-3-(3-(dimethylamino)propyl) carbodiimide hydrochloride (EDC) and *N*-hydroxysuccinimide (NHS) were purchased from GE Healthcare Life Sciences. 1,4,8,11-Tetramethyl-1,4,8,11-tetraazacyclotetradecane (Me4Cyclam, 98%), CuCl (≥99.995%), and $CuCl_2$ (99.999%) were purchased from Sigma-Aldrich and used as received. HBsAg antigen (recombinant, adw subtype) and monoclonal mouse antihepatitis B virus surface antigen antibodies (anti-HBs) were purchased from Hytest (Turku, Finland). Secondary antibodies against mouse antibody (Alexa Fluor 647 Goat Anti-Mouse IgG (H+L)), and against the human antibodies (Alexa Fluor 647 Goat Anti-Human IgG (H+L)) were purchased from Molecular Probes (Eugene, OR, US). Initiator ω-mercaptoundecyl bromoisobutyrate was synthesized according to the literature procedure.[24] The monomers (3-acryloylaminopropyl)-(2-carboxyethyl) dimethylammonium (carboxybetaine methacrylamide, CBMAA) and *N*-(2-hydroxypropyl)methacrylamide (HPMA) were synthesized according to the literature.[25−27] The buffers used were phosphate buffered saline (PBS, 10 mM disodium hydrogen phosphate, 2 mM potassium phosphate, 137 mM sodium chloride, 2.7 mM potassium chloride, pH 7.4), HEPES buffer (10 mM, pH 7.5), and sodium acetate buffer (SA, 10 mM, pH 5).

Biological Samples. Saliva samples were collected from eight healthy donors who were either vaccinated or not-vaccinated against Hepatitis B. The samples were centrifuged for 5 min at 16000*g* and the supernatant was aliquoted. Saliva aliquots were stored at −80 °C before analysis. The donors did not consume food nor liquids for 30 min prior to collecting of samples. The titer of anti-HBs antibodies in serum was tested using enzyme-linked immunoassays (ELISA) done in CE certified laboratory Labors, in Vienna (Austria). The serum was collected from the same donors and at the same time as saliva.

Preparation of Sensor Chips. BK7 glass slides with 2 nm chromium and 50 nm gold films were prepared by high vacuum evaporation. The surface of gold was subsequently rinsed with ethanol and deionized water, dried and cleaned with ozone for 20 min (UVO cleaner, Jelight). Afterward, the gold surface was overnight incubated in a 1 mM solution of ω-mercaptoundecyl bromoisobutyrate in ethanol. This compound served as an initiator in the synthesis of poly(HPMA-*co*-CBMAA) brushes as described in more detail in our previous work.[23] Briefly, for the catalyst solution, 7 mL degassed methanol were transferred (under argon atmosphere) into a Schlenk tube with 354 μmol (35 mg) of CuCl, 78 μmol (10.5 mg) of $CuCl_2$, and 472 μmol (121 mg) of Me_4Cyclam and stirred until complete dissolution. A second Schlenk tube, at 0 °C, contained 16.6 mg (2.4 g) of HPMA and 2.9 mmol (0.7 g) of CBMAA dissolved in 12 mL of degassed water and 5 mL of deoxygenated methanol. The catalyst solution was added using a gastight syringe. Polymerization on the substrates with the initiator SAM was done at 30 °C for 2 h. Samples were washed thoroughly and stored in water until usage.

Immobilization of HBsAg. The antigen HBsAg was immobilized to the brushes via the carboxylate groups carried by CBMAA that were previously activated using the EDC/NHS. First, the brush surface was contacted with SA buffer pH 5. Subsequently, the surface was reacted with a freshly prepared solution 1:1 v/v of EDC (0.4 M) and NHS (0.1 M) for 10 min. Then the surface was rinsed with SA and HEPES buffers for 1 min each and the antigen, HBsAg (25 $\mu g \cdot mL^{-1}$ in HEPES buffer), was flowed over the surface for up to 10 min. Any unreacted active ester groups were let to hydrolyze by flowing PBS for 90 min.

Optical Setup. The time-resolved readout of sandwich assay on the sensor chip was performed by using a setup depicted in Figure 1. It combines angular interrogation of SPR with plasmonically amplified fluorescence detection.

Monochromatic beam with transverse magnetic polarization and a wavelength of λ_{ex} = 633 nm was used to excite SPs on the sensor surface. Intensity of the excitation beam was attenuated to 1.5 μW and it was coupled to a 90° prism made of LASFN9 glass. To the prism base, a sensor chip with gold layer modified by poly(HPMA-*co*-CBMAA) brushes was optically matched by using an immersion oil (from Cargille Inc., USA). A transparent flow-cell (volume 10 μL) was clamped to flow analyzed samples over the surface of the sensor chip at flow rate of 15 $\mu L \cdot min^{-1}$ by

DOI: 10.1021/acs.analchem.6b04432
Anal. Chem. 2017, 89, 2972−2977

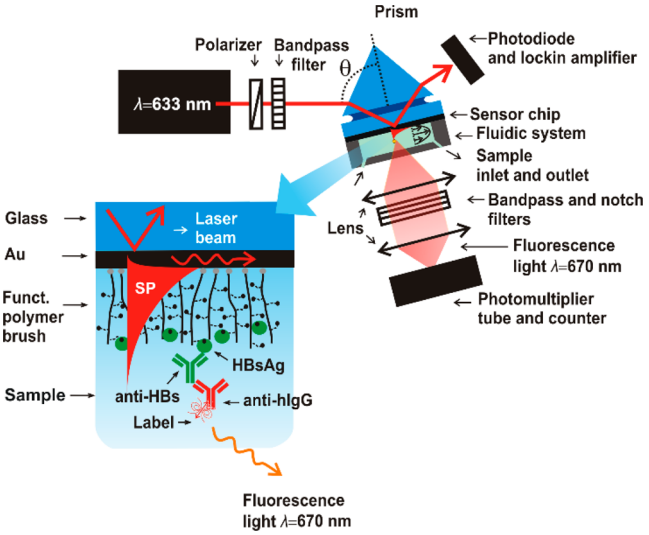

Figure 1. Schematics of plasmon-enhanced fluorescence spectroscopy biosensor with a detail of sensor chip with poly(HPMA-*co*-CBMAA) brush functioning as a binding matrix.

using a peristaltic pump. The angle of incidence of the excitation beam was adjusted to around $\theta \approx 60°$ at which the resonant coupling to SPs at the interface between gold and polymer brushes occurs. The enhanced field intensity of SPs at λ_{ex} excited fluorophore labels on the sensor surface and the fluorescence light emitted at longer wavelength of λ_{em} through the flow cell was collected by a lens with numerical aperture 0.2. The fluorescence beam was focused at the input of a photomultiplier that was connected to a counter. The output fluorescence intensity was recorded in time by using software Wasplas developed at Max Planck Institute for Polymer Research in Mainz (Germany). The fluorophore Alexa Fluor 647 and respective filters were used for the excitation wavelength of λ_{ex} = 633 nm and emission wavelength of λ_{em} = 670 nm. Band pass filter FL632.8−10 from Thorlabs (UK) was employed to select the excitation wavelength λ_{ex} and band-pass filter 670FS10−25 from L.O.T.-Oriel (Germany) and notch filter XNF-632.8−25.0 M from CVI Melles Griot (Germany) were installed for collecting light at emission wavelength λ_{em}. All measurements were carried out at room temperature $T \approx 25$ °C.

RESULTS AND DISCUSSION

Preparation and Characterization of Brushes Architecture. Polymer brushes of poly(HPMA-*co*-CBMAA) were successfully grown from a densely packed SAM of *ω*-mercaptoundecyl bromoisobutyrate on Au via surface initiated atom transfer radical polymerization (SI-ATRP) as described and characterized in detail before.[23] The thickness of the brushes was determined by ellispometry in dry state h_{dry} = 29.2 ± 2.3 nm and when hydrated in water h_{sw} = 81.5 ± 1.7 nm. X-ray photoelectron spectroscopy and Fourier transform infrared grazing angle specular reflectance spectroscopy were utilized to prove the chemical structure of the brushes. The core level C 1s spectrum (Figure 2 a) of the brushes is characterized by C−C, C−H (285.0 eV), C*−C(=O)− from the secondary chemical shifts induced to the carbon atoms in the vicinity to amide and charged carboxylic groups (285.5 eV), C−N (286.1 eV), C−OH (286.9 eV), C(=O)−NH (288.0 eV), and C(=O)−O$^-$ carboxylate (288.7 eV). The high resolution N 1s spectrum of the brushes (Figure 2 b) is characterized by a prevailing amide

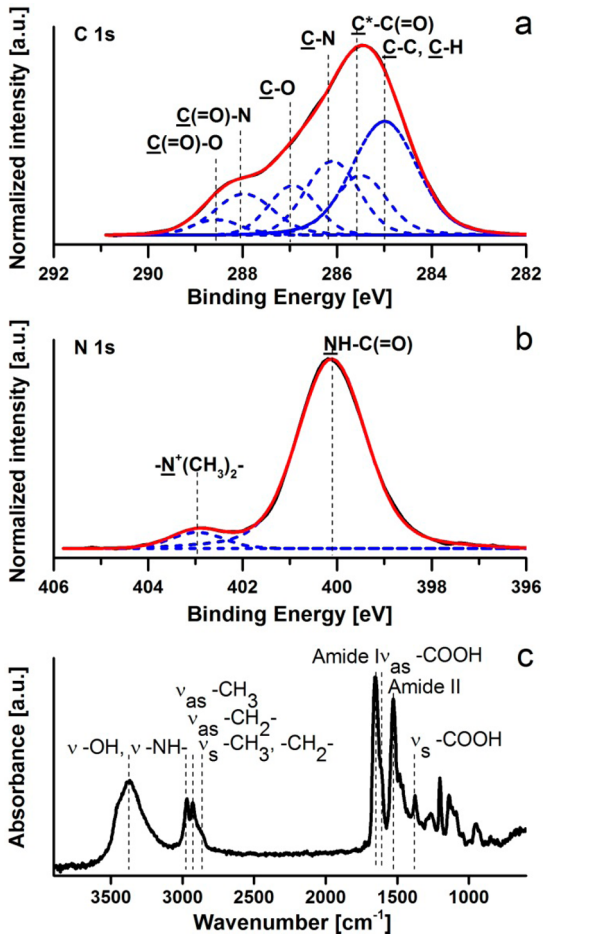

Figure 2. Characterization of the poly(HPMA-*co*-CBMAA) copolymer brush. (a) High resolution of C 1s and (b) N 1s XPS spectra and (c) FTIR GASR spectrum.

contribution (400.1 eV) and a contribution characteristic for the charged quaternary ammonium of the CBMAA comonomer (403.0 eV). The O 1s spectrum is presented in the SI. Further evidence of the chemical composition of the brushes was obtained by FTIR GASR. Figure 2 c depicts the spectrum of poly(HPMA-*co*-CBMAA) brushes which exhibits both a band at 1376 cm^{-1} and a shoulder band at 1610 cm^{-1} corresponding to the symmetric and asymmetric stretching modes of COO$^-$ stemming from CBMAA as well as it shows the amide I and amide II bands at 1527 and 1653 cm^{-1} originating from the HPMA. The morphology of the surface of the brushes was observed using an AFM microscope which can be found in the SI. The functionalization of the gold-coated sensors rendered the surface more hydrophilic as evidenced by the dynamic contact angles of θ_{adv} = 34 ± 0.5°; θ_{rec} = 15.3 ± 3.3.

Selection of an adequate biofunctionalization procedure is of great importance to achieve high loading of immobilized ligands. In particular, the pH of buffer plays a key role as discussed detail in SI. First, carboxylate groups are converted to succinimidyl ester in water and rinsed with SA. The pH of SA buffer (pH 5) is preferred due to the lower rate of hydrolysis of succinimidyl ester compared to alkaline solutions.[28] After the activation of carboxylate groups (negatively charged) of CBMAA to form succinimidyl ester (neutral), using EDC/NHS, the surface becomes positively charged (stemming from quaternary ammonium groups). Therefore, by using a buffer with a pH

DOI: 10.1021/acs.analchem.6b04432
Anal. Chem. 2017, 89, 2972−2977

above the isoelelectric point of the chosen ligand (HBsAg with pI ~4.5)[29] this protein exhibits negative charge and is attracted to the surface by Coulombic force which leads to a higher yield in the immobilization on the brush. After the subsequent rinsing with buffer, the unreacted active esters hydrolyze back to carboxylate groups and the (close to) neutral net charge of the polymer brush is restored. The loading of HBsAg on the brushes was controlled by the reaction time and the herein used chips carried the surface mass density of HBsAg of $\Delta\Gamma = 0.52 \pm 0.03$ $\mu g \cdot cm^{-2}$ as determined by SPR measurements. This value corresponds to about a monolayer as was reported for proteins exhibiting similar molecular weight.[30] Comparable surface mass density has been shown previously for SAM-based architectures, however, the resistance to fouling was largely impaired.[31]

The resistance of the poly(HPMA-*co*-CBMAA) brush to the fouling was evaluated for saliva samples collected from healthy individuals. Since the immobilization of bioreceptors may change the antifouling properties, the fouling of brushes functionalized with HBsAg was evaluated for samples from individuals that showed negative response in the ELISA serum test. As illustrated by SPR sensorgrams in Figure 3, the surface mass density change upon 10 min flow of saliva samples over the sensor surface with and without HBsAg was measured. The protein deposition from undiluted 100% saliva and samples with 10% saliva diluted by PBS was not measurable on pristine poly(HPMA-*co*-CBMAA) brushes, see Figure 3a and Figure 3b.

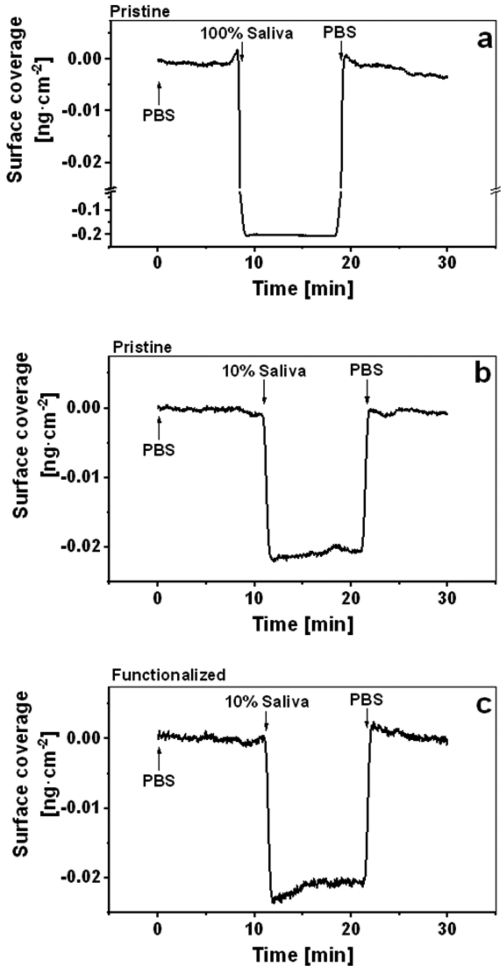

Figure 3. SPR characterization of the fouling on pristine and functionalized poly(HPMA-*co*-CBMAA) brush: (a) Pristine surface in contact with 100% saliva, (b) pristine surface in contact with 10% saliva, and (c) surface modified with HBsAg in contact with 10% saliva.

Importantly, the resistance to the fouling of poly(HPMA-CBMAA) brush is retained even after the HBsAg is immobilized with surface mass density as large as 0.5 $\mu g \cdot cm^{-2}$, see Figure 3c. This is a key observation as the functionalization of brushes composed from individual homopolymers (HPMA and CBMAA) is known to severely deteriorate their antifouling properties.[31] This effect can be ascribed to the reaction of too many functional groups (e.g., carboxyl of CBMAA) leading to a net positive charge or cross-linking of the chains. The herein reported approach enables efficient biofunctionalization of the polymer brush because of the presence of carboxyl groups in CBMAA while preserving antifouling properties of the polymer brush owing to the HPMA units.

Analysis of Clinical Saliva Samples. Clinical saliva samples collected from 8 healthy human donors were used and prepared as described in the methods section. The total amount of sample needed for one analysis was only 15 μL. The response of developed plasmonic biosensor for each saliva sample was compared with the results obtained by ELISA for serum samples from the same donor. The ELISA analysis was carried out by an independent certified laboratory (Labors.at, Vienna, Austria). According to ELISA, the tested saliva samples were obtained from donors that showed negative response in serum (samples D, F, H, antibody titer below the detection limit of ELISA 0.002 IU·mL^{-1}), positive response in serum (B, E, G, 0.068−0.645 IU·mL^{-1}) and highly positive response (A, C, > 1 IU·mL^{-1}).

The SPR detection principle was tested for the analysis of saliva samples collected from donors which were known to exhibit highly positive response in serum. These serum samples were analyzed by using an identical instrument with the same brush surface architecture.[23] While the direct binding of anti-HBs human IgG could be easily observed from serum samples, no measurable positive response was obtained from saliva samples, even after binding of secondary antibody against human IgG (hIgG). Therefore, the PEF biosensor was used in order to increase the sensitivity as described further.

The developed PEF assay is illustrated in Figure 4. First, a stable baseline in fluorescence signal acquired in time was established upon a flow of PBS over the surface of HBsAg-functionalized brushes. Then a calibration step was performed in which PBS spiked with mouse anti-HBs was flowed at 10 pM concentration through the sensor for 10 min. This antibody was labeled with Alexa Fluor 647 dye and therefore the injection is

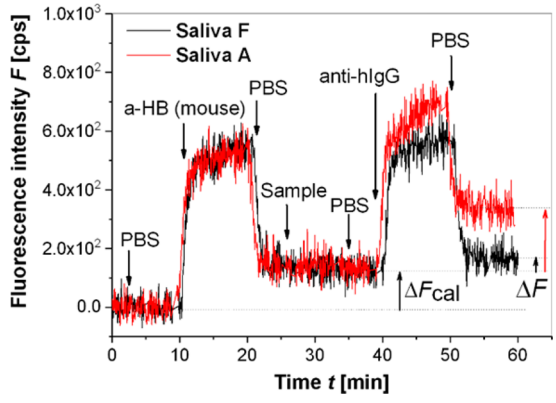

Figure 4. Example of kinetics of fluorescence signal for negative and highly positive saliva samples.

DOI: 10.1021/acs.analchem.6b04432
Anal. Chem. 2017, 89, 2972−2977

accompanied by increased fluorescence signal F. The sensorgram in Figure 4 shows that an abrupt change occurs at time t = 10 min due to the excitation of fluorophores present in the bulk. Between the time t = 10 and 20 min, a gradual increase in the signal occurs because of the affinity binding to the immobilized antigen HBsAg. At time t = 20 min the sensor surface is rinsed with buffer and the fluorescence signal drops to an increased level ΔF_{cal} which is proportional to the amount of affinity bound anti-HBs molecules.

After 5 min rinsing, an analyzed 10% saliva sample was flowed over the sensor surface for 10 min. At this time no fluorescence change is observed as the human hIgG specific to HBsAg are not labeled. To detect the presence of these antibodies on the surface, the sensor was rinsed for 5 min with PBS and the antihuman IgG labeled with Alexa Fluor 647 dye (anti-hIgG, 4 $\mu g \cdot mL^{-1}$ in PBS) was injected. This compound was flowed for 10 min between t = 40 and 50 min. Similarly as in the calibration step, the fluorescence signal rapidly increased upon the injection and then gradually rose due to the affinity binding to captured hIgG. An additional rinsing with PBS for 5 min was applied and the difference in the fluorescence intensity ΔF before and after the flow of detection anti-hIgG was determined. In order to compensate for small changes in the alignment, the sensor response was defined as a ratio $\Delta F/\Delta F_{cal}$.

Figure 5a compares the obtained normalized fluorescence response $\Delta F/F_{cal}$ for saliva samples with values determined by ELISA for serum. The PEF saliva analysis was performed in triplicate for each sample and showed error bars represent the standard deviation (SD) of measured values. The average SD

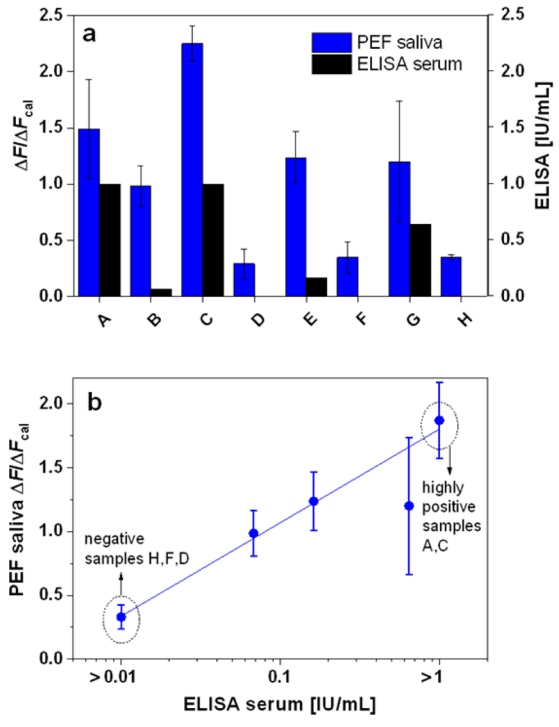

Figure 5. (a) Comparison of the response of PEF biosensor to saliva samples collected from donors A-H compared to ELISA-based characterization of respective serum samples. (b) Overview of PEF sensor response as a function of concentration in serum as determined by ELISA. Indicated errors represent standard deviation for samples measured in triplicate, the response and error to negative and highly positive samples is averaged, line shows a linear fit with r-square (COD) value of 0.89.

associated with chip-to-chip variations of the PEF assay output is 26% of the mean value of fluorescence response $\Delta F/F_{cal}$. This relatively high error can be partially ascribed to the noise in the detected fluorescence signal (as observed in Figure 4) which can be improved by using plasmon-enhanced fluorescence schemes with higher enhancement factor and thus improved signal-to-noise ratio.[32,33] In addition, the reproducibility of the assay that involves multiple manually performed steps including saliva centrifugation, dilution of supernatant with buffer, sensor calibration with labeled mouse IgG, and sequential flow of saliva sample and labeled antihuman IgG may be improved by using automatized flow injection system. The plotted dependence of PEF saliva response on respective ELISA serum response in Figure 5b shows that it can be fitted with a linear function (r-square value of 0.89, the ELISA response is presented in log scale on the horizontal axis). In this graph, the response for samples collected from negative donors (H, F, D) and highly positive donors (A, C) was averaged. The results of PEF analysis of saliva samples indicate that highly positive saliva samples (average fluorescence response of 1.87, SD = 0.3) can be reliably discriminated from negative samples (average fluorescence response of 0.33, SD = 0.1). Interestingly, the PEF response to saliva samples is not proportional to that acquired by ELISA for serum samples as the slope of the respective dependence in a log−log representation substantially differs from 1 (is of about 0.3). Therefore, such dependence in conjunction with relatively high error bars does not allow for accurate quantitative measurements in the range between 0.01 and 1 $IU \cdot mL^{-1}$. The reason for such deviations may be attributed to different composition of saliva compared to serum which may affect the assay. In addition, we assume that the hIgG antibodies present in saliva and serum can bind to HBsAg with a range of affinity constants. As in ELISA the immobilized antigen is typically incubated for much longer time (hours) compared to the presented PEF sensor (10 min), the lower affinity fraction of hIgG against HBsAg may not be detected by the PEF biosensor while in ELISA it can contribute to the sensor signal.

CONCLUSIONS

We report for the first time the successful implementation of a plasmonic biosensor for the analysis of human IgG against hepatitis B surface antigen in clinical saliva samples. The work pursued enhanced specificity and sensitivity to analyze minute amounts of biomarkers in the complex saliva matrix. This was achieved by the design of a novel antifouling biointerface architecture based on poly(HPMA-*co*-CBMAA) brushes in combination with surface plasmon-enhanced fluorescence detection principle. It is worth of noting that regular SPR biosensor with identical surface architecture and assay did not show measurable signal for analyzed clinical saliva samples and made the use of plasmonically enhanced fluorescence detection principle necessary. The biosensor showed excellent resistance to fouling from saliva samples and allowed distinguishing of highly positive clinical saliva samples (respective serum ELISA response >1 IU/mL) and negative clinical saliva samples (respective serum ELISA response <0.01 IU/mL). It is envisioned that the achieved results will pave the way to new class of biosensor technologies that can be deployed outside centralized laboratories and which take advantage of the analysis of bodily fluids that are collected completely noninvasively. In conjunction with miniaturized PEF readers[34] and more sensitive plasmonic architectures[32,33] the presented approach is among others

DOI: 10.1021/acs.analchem.6b04432
Anal. Chem. 2017, 89, 2972−2977

expected to find its applications in clinical practices for diagnosis and measuring of the antibody titers.

■ ASSOCIATED CONTENT

Supporting Information

The Supporting Information is available free of charge on the ACS Publications website at DOI: 10.1021/acs.analchem.6b04432.

Characterization of poly(HPMA-*co*-CBMAA) brushes by using X-ray photoelectron spectroscopy (XPS), Fourier transform infrared grazing angle specular reflectance spectroscopy (FTIR-GASR), and atomic force microscopy (AFM) (PDF)

■ AUTHOR INFORMATION

Corresponding Authors

*E-mail: riedel@imc.cas.cz. Phone: +420 296 809 333. Fax: +420 296 809 410.
*E-mail: rodriguez@dwi.rwth-aachen.de. Phone: +49 241 8023362. Fax: +49 241 80 23301.
*E-mail: jakub.dostalek@ait.ac.at. Phone: +43 (0) 50550 4470. Fax: +43 (0) 50550 4450.

ORCID

Cesar Rodriguez-Emmenegger: 0000-0003-0745-0840
Jakub Dostálek: 0000-0002-0431-2170

Author Contributions

The manuscript was written through contributions of all authors. All authors have given approval to the final version of the manuscript.

Funding

T.R., E.B., F.S., and O.P.-G. are grateful for the support from the Grant Agency of the Czech Republic (GACR) under Contract No. 15-09368Y and P205-12-G118, the Ministry of Education, Youth and Sports of CR within the National Sustainability Program II (Project BIOCEV-FAR LQ1604), by the project "'BIOCEV'" (CZ.1.05/1.1.00/02.0109) and by OPPK (CZ.2.16/3.1.00/21545), from the European Regional Development Fund. SH and JD were supported by Austrian Science Fund (FWF) through the project ACTIPLAS (P 244920-N20), and FEMTECH Frauen in Forschung and Technologie Initiative of the Austrian Ministry for Transportation, Innovation and Technology No. 840988. C.R.-E. acknowledges support of the Center for Chemical Polymer Technology (CPT) under the support of the EU and the federal state of North Rhine-Westphalia (Grant EFRE 30 00 883 02).

Notes

The authors declare no competing financial interest.

■ REFERENCES

(1) Lee, Y.-H.; Wong, D. T. *Am. J. Dent.* **2009**, *22*, 241−248.
(2) Rehak, N. N.; Cecco, S. A.; Csako, G. *Clin. Chem. Lab. Med.* **2000**, *38*, 335−343.
(3) Patil, P. B.; Patil, B. R. *J. Indian Soc. Periodontol.* **2011**, *15*, 310−317.
(4) Rathnayake, N.; Åkerman, S.; Klinge, B.; Lundegren, N.; Jansson, H.; Tryselius, Y.; Sorsa, T.; Gustafsson, A. *PLoS One* **2013**, *8*, e61356.
(5) Gitlin, N. *Clinical Chemistry* **1997**, *43*, 1500−1506.
(6) Schweitzer, A.; Horn, J.; Mikolajczyk, R. T.; Krause, G.; Ott, J. J. *Lancet* **2015**, *386*, 1546−1555.
(7) Lozano, R.; Naghavi, M.; Foreman, K.; Lim, S.; Shibuya, K.; Aboyans, V.; Abraham, J.; Adair, T.; Aggarwal, R.; Ahn, S. Y.; et al. *Lancet* **2012**, *380*, 2095−2128.
(8) Nopporpanth, S.; Sathirapongsasuti, N.; Chongsrisawat, V.; Poovorawan, Y. *Southeast Asian J. Trop. Med. Public Health* **2000**, *31*, 419−421.
(9) Brandtzaeg, P. *Ann. N. Y. Acad. Sci.* **2007**, *1098*, 288−311.
(10) Patidar, K. A.; Parwani, R. N.; Wanjari, S. P. *J. Oral Sci.* **2011**, *53*, 97−102.
(11) Chiappin, S.; Antonelli, G.; Gatti, R.; De Palo, E. F. *Clin. Chim. Acta* **2007**, *383*, 30−40.
(12) Homola, J. *Chem. Rev.* **2008**, *108*, 462−493.
(13) Stewart, M. E.; Anderton, C. R.; Thompson, L. B.; Maria, J.; Gray, S. K.; Rogers, J. A.; Nuzzo, R. G. *Chem. Rev.* **2008**, *108*, 494−521.
(14) Khatua, S.; Paulo, P. M.; Yuan, H.; Gupta, A.; Zijlstra, P.; Orrit, M. *ACS Nano* **2014**, *8*, 4440−4449.
(15) Liebermann, T.; Knoll, W. *Colloids Surf., A* **2000**, *171*, 115−130.
(16) Lakowicz, J. R.; Ray, K.; Chowdhury, M.; Szmacinski, H.; Fu, Y.; Zhang, J.; Nowaczyk, K. *Analyst* **2008**, *133*, 1308−1346.
(17) Choi, Y.-H.; Lee, G.-Y.; Ko, H.; Chang, Y. W.; Kang, M.-J.; Pyun, J.-C. *Biosens. Bioelectron.* **2014**, *56*, 286−294.
(18) Zheng, S.; Kim, D.-K.; Park, T. J.; Lee, S. J.; Lee, S. Y. *Talanta* **2010**, *82*, 803−809.
(19) Helton, K. L.; Nelson, K. E.; Fu, E.; Yager, P. *Lab Chip* **2008**, *8*, 1847.
(20) Blaszykowski, C.; Sheikh, S.; Thompson, M. *Biomater. Sci.* **2015**, *3*, 1335−1370.
(21) Chung, J. W.; Kim, S. D.; Bernhardt, R.; Pyun, J. C. *Sens. Actuators, B* **2005**, *111*−*112*, 416−422.
(22) Rodriguez-Emmenegger, C.; Hasan, E.; Pop-Georgievski, O.; Houska, M.; Brynda, E.; Alles, A. B. *Macromol. Biosci.* **2012**, *12*, 525−532.
(23) Riedel, T.; Surman, F.; Hageneder, S.; Pop-Georgievski, O.; Noehammer, C.; Hofner, M.; Brynda, E.; Rodriguez-Emmenegger, C.; Dostálek, J. *Biosens. Bioelectron.* **2016**, *85*, 272−279.
(24) Jones, D. M.; Brown, A. A.; Huck, W. T. S. *Langmuir* **2002**, *18*, 1265−1269.
(25) Rodriguez-Emmenegger, C.; Schmidt, B. V.; Sedlakova, Z.; Subr, V.; Alles, A. B.; Brynda, E.; Barner-Kowollik, C. *Macromol. Rapid Commun.* **2011**, *32*, 958−965.
(26) Rodriguez-Emmenegger, C.; Houska, M.; Alles, A. B.; Brynda, E. *Macromol. Biosci.* **2012**, *12*, 1413−1422.
(27) Ulbrich, K.; Šubr, V.; Strohalm, J.; Plocová, D.; Jelínková, M.; Říhová, B. *J. Controlled Release* **2000**, *64*, 63−79.
(28) Hermanson, G. T. In *Bioconjugate Techniques*, 3rd ed.; Academic Press: Boston, 2013; pp 229−258.
(29) Lee, Y. S.; Kim, B. K.; Choi, E. C. *Arch. Pharmacal Res.* **1998**, *21*, 521−526.
(30) Vaisocherová-Lísalová, H.; Surman, F.; Víšová, I.; Vala, M.; Špringer, T.; Ermini, M. L.; Šípová, H.; Šedivák, P.; Houska, M.; Riedel, T. s.; et al. *Anal. Chem.* **2016**, *88*, 10533−10539.
(31) Vaisocherová, H.; Ševců, V.; Adam, P.; Špačková, B.; Hegnerová, K.; de los Santos Pereira, A.; Rodriguez-Emmenegger, C.; Riedel, T.; Houska, M.; Brynda, E.; Homola, J. *Biosens. Bioelectron.* **2014**, *51*, 150−157.
(32) Bauch, M.; Dostalek, J. *Opt. Express* **2013**, *21*, 20470−20483.
(33) Wang, Y.; Brunsen, A.; Jonas, U.; Dostálek, J.; Knoll, W. *Anal. Chem.* **2009**, *81*, 9625−9632.
(34) Toma, K.; Adam, P.; Vala, M.; Homola, J.; Knoll, W.; Dostalek, J. *Opt. Express* **2013**, *21*, 10121−10132.

DOI: 10.1021/acs.analchem.6b04432
Anal. Chem. 2017, 89, 2972−2977